



# A parametric study of the lensing properties of dodecagonal photonic quasicrystals<sup>☆</sup>

E. Di Gennaro <sup>a,\*</sup>, D. Morello <sup>b</sup>, C. Miletto <sup>a</sup>, S. Savo <sup>a</sup>,  
A. Andreone <sup>a</sup>, G. Castaldi <sup>b</sup>, V. Galdi <sup>b</sup>, V. Pierro <sup>b</sup>

<sup>a</sup> CNISM and Department of Physics, University of Naples “Federico II”, Piazzale Tecchio 80, I-80125 Napoli, Italy

<sup>b</sup> Waves Group, Department of Engineering, University of Sannio, Corso Garibaldi 107, I-82100 Benevento, Italy

Received 28 June 2007; received in revised form 17 October 2007; accepted 5 December 2007

Available online 14 December 2007

## Abstract

We present a study of the lensing properties of two-dimensional (2-D) photonic quasicrystal (PQC) slabs made of dielectric cylinders arranged according to a 12-fold-symmetric square-triangle aperiodic tiling. Our full-wave numerical analysis confirms the results recently emerged in the technical literature and, in particular, the possibility of achieving focusing effects within several frequency regions. However, contrary to the original interpretation, such focusing effects turn out to be critically associated to local symmetry points in the PQC slab, and strongly dependent on its thickness and termination. Nevertheless, our study reveals the presence of some peculiar properties, like the ability to focus the light even for slabs with a reduced lateral width, or beaming effects, which render PQC slabs potentially interesting and worth of deeper investigation.

© 2007 Elsevier B.V. All rights reserved.

PACS : 42.70.Qs; 41.20.Jb; 61.44.Br; 42.30.-d

Keywords: Photonic quasicrystals; Negative refraction; Superlensing

## 1. Introduction

Photonic crystals (PCs), featuring a periodically modulated refractive index, represent an active research area since nearly two decades [1,2]. The strong interest toward these structures is motivated by their capability of inhibiting the spontaneous emission of light, which potentially renders them the building-block components of an all-optical circuitry [3].

In PCs, multiple wave scattering at frequencies near the Bragg condition prevents propagation in certain

directions, producing a *bandgap*. Anomalous (even negative) refraction and subwavelength focusing (“superlensing”) properties for PCs have been theoretically predicted (see, e.g., [4–7]) and experimentally verified (cf. [8,9]). The theoretical foundations of the (analytic and numerical) modeling, prediction, and physical understanding of the above phenomena are based on well-established tools and concepts developed for the study of wave dynamics in *periodic* structures, such as Bloch theorem, unit cell, Brillouin zone, equifrequency surfaces (EFS), etc.

With specific reference to lensing applications, two different approaches have been presented to obtain subwavelength resolution using a PC slab. The first one assumes that, under suitable conditions (single beam propagation, negative group velocity in the specific

<sup>☆</sup> This paper was presented at the PECS VII Conference.

\* Corresponding author. Tel.: +39 081 7682661;  
fax: +39 081 2391821.

E-mail address: emiliano@na.infn.it (E. Di Gennaro).

frequency band, and circular EFS), a PC can behave like a homogeneous material with a negative refractive index  $n = -1$ . These features are likely found near a frequency band edge and in the case of high dielectric contrast [4]. Furthermore, modifying the slab terminations, the impedance mismatch with the surrounding medium can be minimized [10] and/or surface waves can be excited allowing (partial) reconstruction of evanescent waves [11]. Such a slab is not a perfect lens [12], in the sense that the image has a finite resolution, since not all evanescent components can be restored. Nevertheless, the focus position follows the simple ray-optical construction as for a flat lens with  $n = -1$  [6,13]. The second approach relaxes some of the previous requirements (negative group velocity and isotropic refraction properties) and achieves “all-angle negative refraction” (AANR) without an effective negative index, provided that the EFS are all convex and larger than the frequency contour pertaining to the surrounding medium [7]. This condition is still sufficient for a PC slab to focus with subwavelength resolution, if the termination is designed so as to sustain surface modes. It is worth noticing that, in this case, the focus position does not follow the ray-optical construction [14] and is *restricted* [13].

Recently, there has been an increasing interest toward the study of *aperiodically ordered* PCs. Such structures are inspired by the “quasicrystals” in solid-state physics [15,16] and the related theory of “aperiodic tilings” [17], and are accordingly referred to as “photonic quasicrystals” (PQCs). Like their solid-

state physics counterparts, PQC structures can exhibit long-range (e.g., quasiperiodic) order and weak (e.g., statistical and/or local) rotational symmetries which are not bounded by the crystallographic restriction and can thus be considerably *higher* than those achievable in periodic PCs [18]. Accordingly, it has been proposed to utilize PQC structures in order to maintain the periodic-like scattering of light, while introducing additional geometric degrees of freedom potentially useful for performance control and optimization. However, it must be said that the lack of periodicity renders the study of PQCs very complex and computationally-demanding. Although some concepts developed for periodic PCs can be used for the analysis of the properties of PQCs [19,20], a rigorous extension of a Bloch-type theorem (and associated tools and concepts) does not exist.

Recent studies of the EM properties of 8-fold [21], 10-fold [19,22] and 12-fold [18] PQCs have shown that a gap in the density of states, accompanied by significant dips in the transmission spectra, can be achieved. PQCs also allow, in principle, for a higher degree of flexibility and tunability for defect-type [23,24] and intrinsic [25] localized modes. Moreover, examples of subwavelength focusing properties have been presented for 2-D PQCs exhibiting various (8-fold, 10-fold, and 12-fold) rotational symmetries [26,27]. Similar results were also obtained in the case of acoustic waves [28].

Although the above studies on the focusing properties of PQC slabs reveal some appealing properties, such as polarization-insensitive and non-near-field imaging, we believe that the original phenomenology

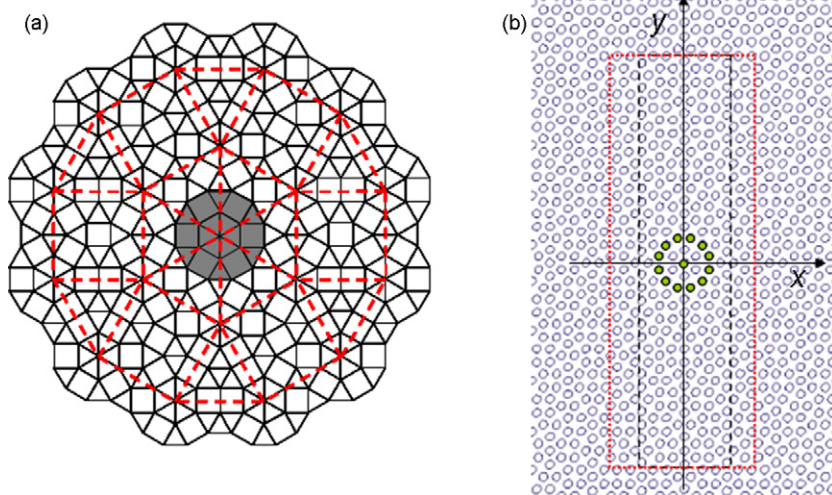


Fig. 1. Dodecagonal PQC geometry. (a) Illustration of the Stampfli inflation rule. The gray-shaded dodecagon in the center represents the parent tiling from which a big parent (red dashed lines) is generated by applying a scaling factor  $v = \sqrt{3} + 2$ . (b) Two examples of PQC slabs of different thickness (black-dashed and red-dotted rectangles) extracted from the tiling. The green-full-dots dodecagon in the center corresponds to the parent tiling in (a).

interpretation provided in [26], within the framework of “effective negative refractive-index and evanescent wave amplification”, is questionable and deserves a deeper investigation. In this paper, we present some representative results from a comprehensive parametric study of the focusing properties of 12-fold symmetric PQC slabs (as in [26]), based on full-wave numerical simulations (Fourier–Bessel multipolar expansion). In particular, with reference to the line-source imaging scenario, we investigate the critical role of the global vs. local symmetry of the lattice (which is merely glossed over in [27]), by varying the PQC slab thickness, lateral

width, and termination, as well as the source position in both parallel and orthogonal directions with respect to the slab surface.

## 2. Samples and methods

As in [26], the 2-D PQC of interest is made of infinitely-long dielectric cylinders with relative permittivity  $\epsilon_r = 8.6$  and radius  $r = 0.3a$  placed (in vacuum) at the vertices of a 12-fold-symmetric aperiodic tiling with lattice constant (tile side-length)  $a$ , generated by the so-called Stampfli inflation rules [29] illustrated in Fig. 1(a).

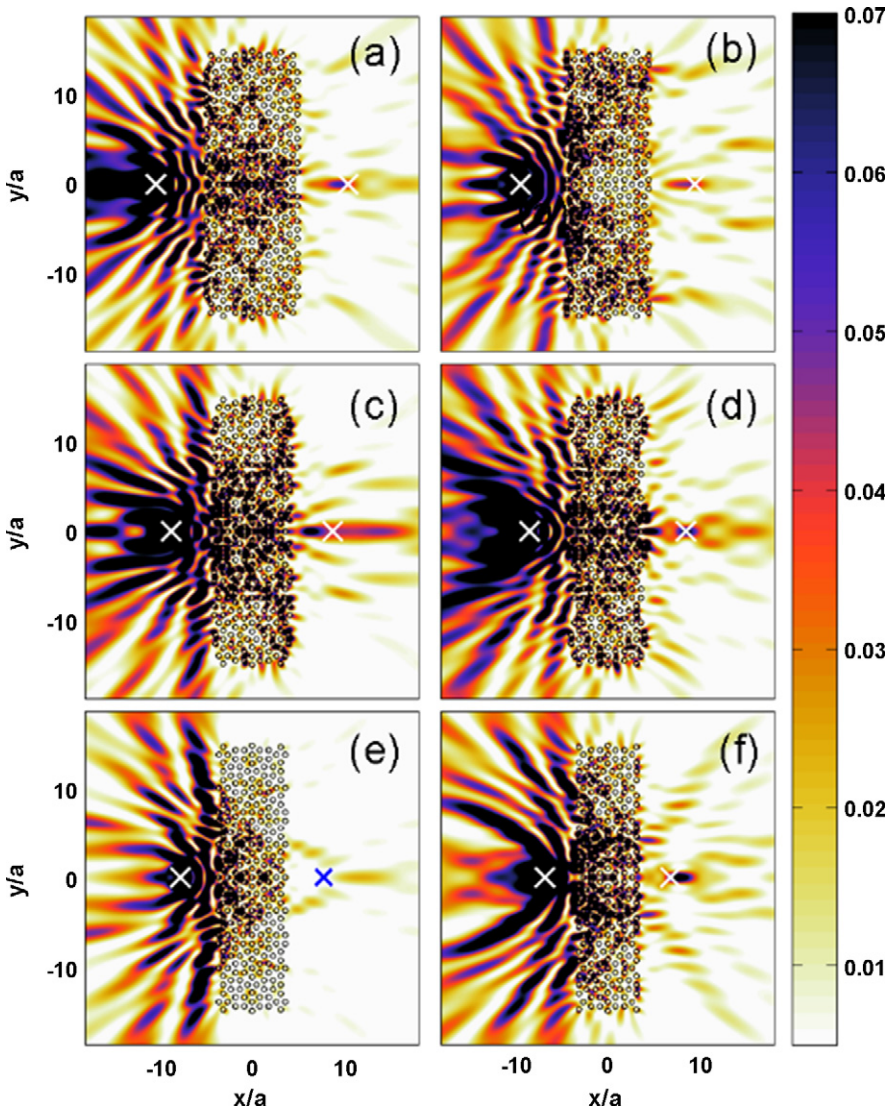


Fig. 2. Intensity field maps for various symmetric slab configurations with different values of the thickness  $t$ . (a)  $t = 11a$ ; (b)  $t = 9.8a$ ; (c)  $t = 9a$ ; (d)  $t = 8.8a$ ; (e)  $t = 8a$  and (f)  $t = 7a$ . An electric line-source is placed at  $y = 0$  and a distance  $d_x = t/2$  from the vacuum–slab interface. The crosses mark the source position and the ray-optical ( $n = -1$ ) prediction for the focus location. The color-scale limits in the plots are chosen so as to properly reveal details in the internal and external fields that would be otherwise overwhelmed by the dominant features.

The (recursive) generation algorithm is based on a parent tiling represented by the central gray-shaded dodecagon. Scaling up this structure by an inflation factor  $\nu = \sqrt{3} + 2$ , one obtains a big parent (red dashed dodecagon in Fig. 1(a)). Copies of the original tiling are subsequently placed at each vertex of the big parent, and the process is iterated up to the desired tiling extension. From a suitably-sized tiling, we extract several PQC slabs of different sizes, with a thickness  $t$  (along the  $x$ -axis) ranging between  $\sim 7a$  and  $\sim 11a$  (see the two rectangles in Fig. 1(b), corresponding to the two examples presented in [26]) and a lateral width  $h$  (along the  $y$ -axis) varying between  $\sim 11a$  and  $\sim 30a$ . Our numerical simulations are carried out via a 2-D full-wave method based on a multipolar expansion of the fields around (and inside)

each cylinder [30]. This method is closely related to the Korringa–Kohn–Rostocker method used in solid-state physics [31] (which is itself derived from a pioneering work by Lord Rayleigh in electrostatics [32]), and has also been recently applied to the study of the local density of states in finite-size PCs [33,34] and PQCs [22]. In the present investigation, only E-type polarization is considered, i.e. the electric field is assumed to be parallel to the cylinders.

### 3. Representative results

As a preliminary step, we studied the focusing properties of the two PQC slabs in Fig. 1(b), for a fixed line-source position, and varying the normalized

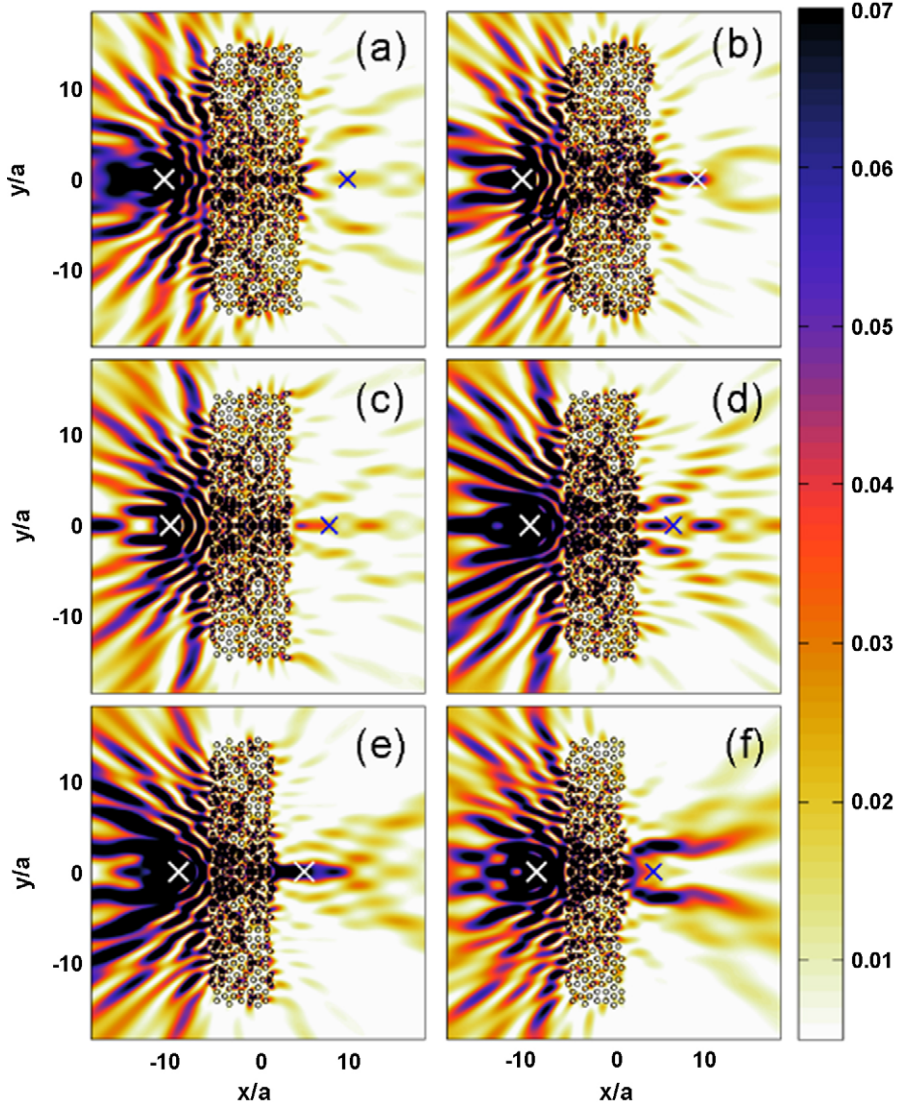


Fig. 3. As in Fig. 2, but for asymmetric configurations. (a)  $t = 10.3a$ ; (b)  $t = 9.8a$ ; (c)  $t = 9a$ ; (d)  $t = 8a$ ; (e)  $t = 7a$  and (f)  $t = 6.6a$ .

frequency  $a/\lambda$  (with  $\lambda$  being the vacuum wavelength) within a range between the first and second bandgaps ( $0.354 \leq a/\lambda \leq 0.533$ ). We found several frequency regions (including those in [26]) where a clear focus was visible. We note that this feature represents a first remarkable difference with the PC case, where the focusing regions tend to be more rare and well separated. In PQCs, likely due to their inherent self-similar nature [20], focusing effects seem to occur more densely in the spectrum. In all simulations below, attention is focused on the normalized frequency  $a/\lambda = 0.394$ , corresponding to the value for which a refractive behavior emulating a homogeneous medium with  $n = -1$  was estimated in [26].

### 3.1. Effects of slab thickness

In order to gain some insight into the focusing properties, we then considered PQC slabs of different thickness. The line-source was always placed at a distance  $d_x = t/2$  from the vacuum–slab interface, and in correspondence of the center of the parent tiling ( $y = 0$ ). From a simple ray-optical construction (for flat lenses

with  $n = -1$ ), the focus is accordingly expected to be located in a symmetric position with respect to the slab. The slab thickness was changed by removing cylinders in such a way to preserve the inversion symmetry with respect to the  $y$ -axis, thereby obtaining six different configurations, which include as extremes the two samples shown in Fig. 1(b). As a first result, our simulations confirmed the results in [26], as shown in the (intensity) field maps in Fig. 2(a) and (f). A focus is clearly observable at a position very close to the ray-optical prediction (marked by a cross symbol). However, for intermediate thickness (see Fig. 2(b)–(e)), the focusing properties become rather questionable. Moreover, in all the simulations, the reflection coefficient in the source plane is considerably nonzero, indicating the presence of a significant impedance mismatch at the vacuum–slab interface. Furthermore, the field distributions inside the slab turn out to be significantly different, suggesting a strong dependence from the whole slab configuration, including its termination. In this connection, we note that it is not possible to change the PQC slab thickness without changing at least one termination. In Fig. 2(c) and (d), a feature that resembles a “beaming

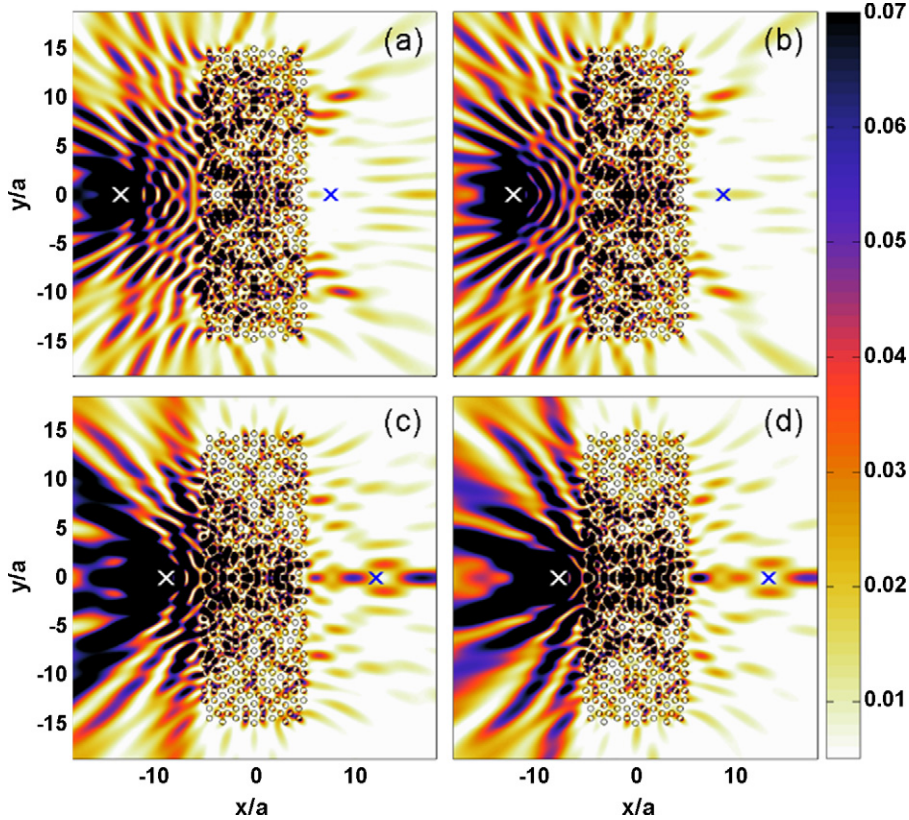


Fig. 4. As in Fig. 2(a) (i.e., thicker slab, cf. red dotted rectangle in Fig. 1(b)), but for various source distances  $d_x$  from the vacuum–slab interface. (a)  $d_x = 8.3a$ ; (b)  $d_x = 7.1a$ ; (c)  $d_x = 3.6a$  and (d)  $d_x = 2.5a$ . The source  $y$ -position is maintained at  $y = 0$ .

effect" can be observed, together with a strong field intensity along the vacuum–slab interface on the image side. In periodic PC slabs, such a phenomenon has been related to the presence of localized photon states on the slab surface [7], stemming from an *overall resonance* in the structure.

In Fig. 3, the field maps pertaining to other six different PQC slabs of various thickness are displayed. In these examples, the slab thickness was changed by removing dielectric cylinders only from the image side, thereby destroying the inversion symmetry with respect to the  $y$ -axis. Also in this case, the field distribution on the image side appears to depend critically on the structure geometry. Although a clear single focus cannot be identified, several spots (Fig. 3(a) and (d)), or beaming effects (Fig. 3(b), (e), and (f)) are visible, indicating that the inversion symmetry does play a key role in the focus formation.

### 3.2. Effects of source position

We then fixed the slab geometry to that of Fig. 2(a) (thicker slab), that was found to exhibit focusing

properties, and changed the source position. In case of a flat lens with  $n = -1$ , simple ray-optics predicts the source-image distance to remain constant and equal to twice the lens thickness [6]. Results for periodic PCs showing an almost isotropic refractive response (see, e.g., [13]) agree fairly well with this prediction. First, we kept the source in a symmetric position along the transverse direction ( $y = 0$ ), varying the distance  $d_x$  from the slab from  $0.75a$  up to  $10.5a$ . In Fig. 4, some representative field maps are shown. A variety of effects are observed, ranging from the absence of focus (Fig. 4(a)) to multiple spots (Fig. 4(c) and (d)), but always in the near-field region, raising further concerns about the interpretation in [26]. Similar results [14] were also observed for PCs, in the case of an anisotropic regime with positive or negative refraction properties, where the near-field focusing was found to be dominated by a self-collimation effect.

Next, for a fixed source-slab distance  $d_x = t/2$ , we moved the source parallel to the vacuum–slab interface. Representative results are shown in Fig. 5. In PCs, for source displacements that preserve the distance from the slab and the structure periodicity, the focus remains

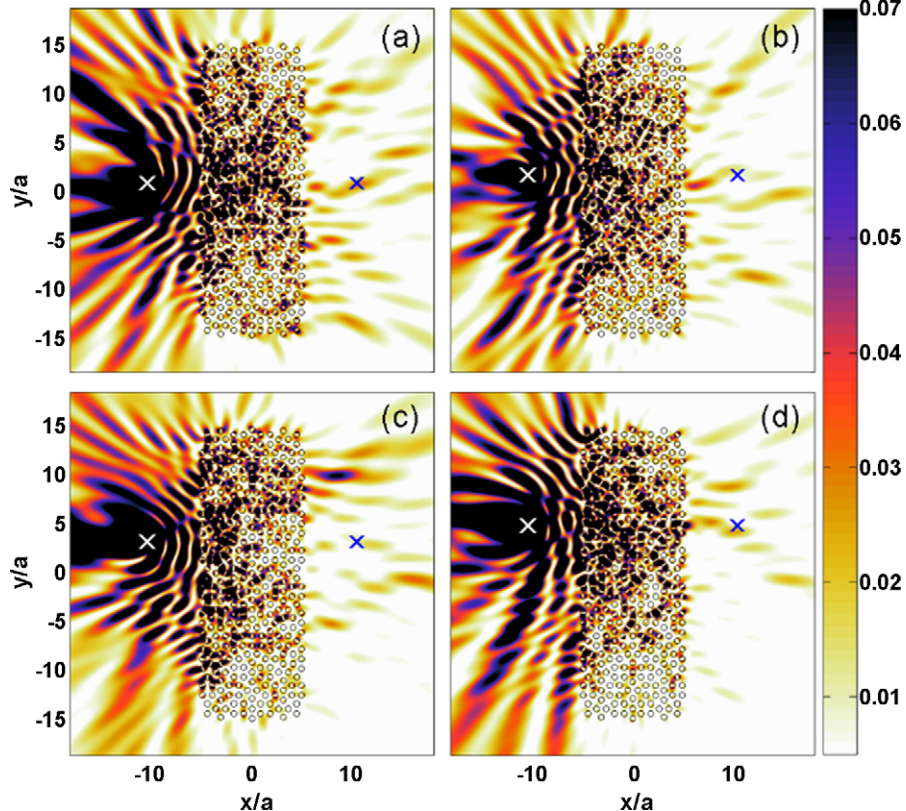


Fig. 5. As in Fig. 4, but for various source displacements  $d_y$  along the  $y$ -axis. (a)  $d_y = 0.75a$ ; (b)  $d_y = 1.5a$ ; (c)  $d_y = 3a$  and (d)  $d_y = 6a$ . The source distance from the vacuum–slab interface is maintained at  $d_x = 5.5a$  (i.e., half the slab thickness).

unaffected, and its position follows the source location. Conversely, in our PQC case, when the  $x$ -axis symmetry is broken, the focus undergoes a rapid deterioration, and is completely destroyed for a source displacement of  $d_y = 6a$  (see Fig. 5(d)). These findings highlight the importance of keeping the source on the same axis of the central symmetry point in the 12-fold tiling (highlighted in Fig. 1(b)), as also observed in [27]. For the thicker slab configuration in Fig. 1(b), we also performed some simulations involving a collimated Gaussian-beam impinging on three different points of the PQC slab interface with three different incidence angles. Results shown in Fig. 6, displaying complex

multi-beam features in the transmitted field that are strongly dependent on the incidence point, highlight the absence of a clear-cut refractive behavior, and explain the strong dependence of the focusing effects on the source distance from the slab (cf. Fig. 4) and lateral displacement (cf. Fig. 5).

### 3.3. Effects of slab lateral width

To better illustrate the role of the local symmetry point, we also varied the slab lateral width asymmetrically (i.e., removing cylinders only from one side of the  $y$ -axis) while keeping the source in the central

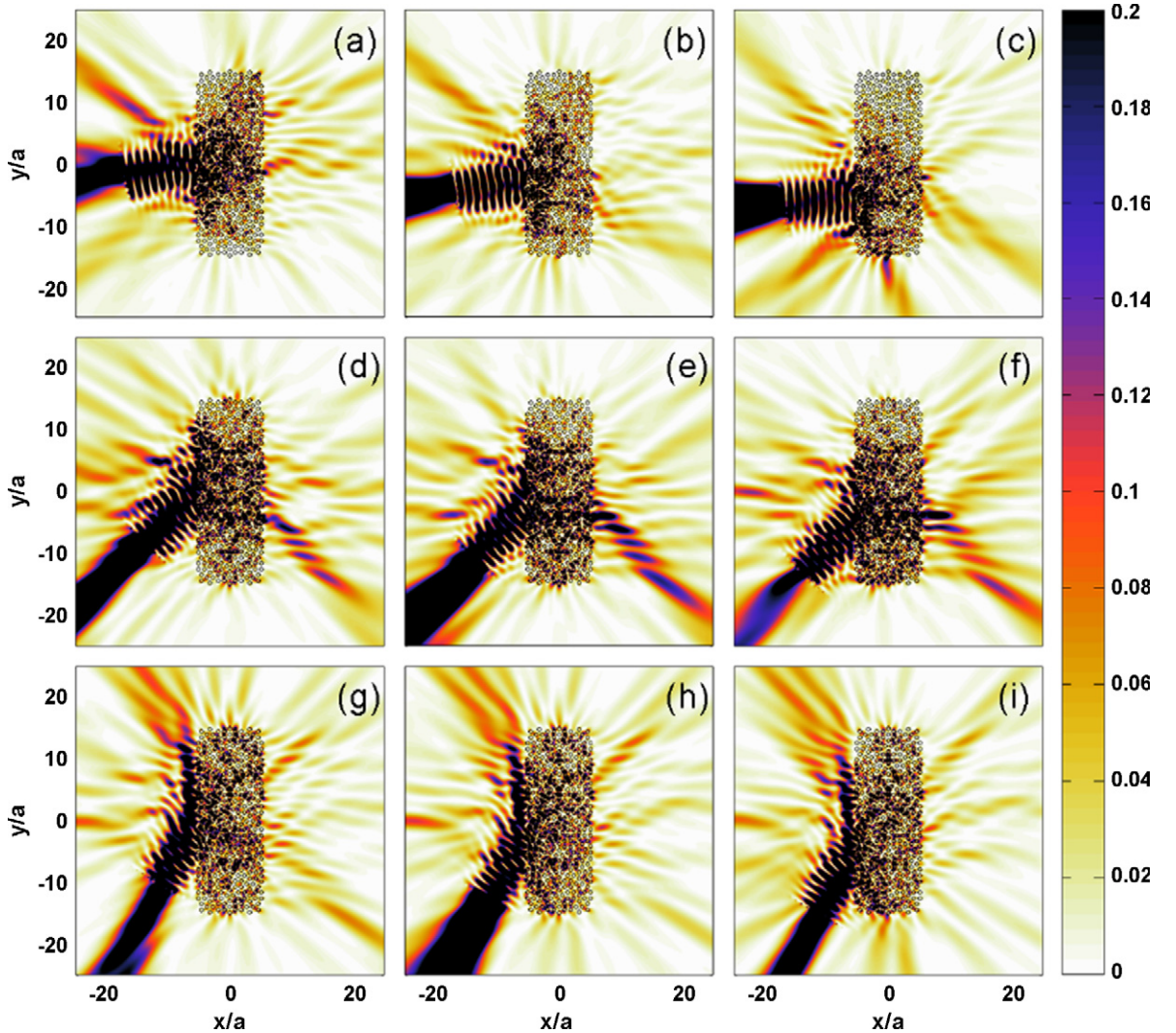


Fig. 6. As in Fig. 2(a), but for Gaussian-beam incidence at various lateral positions  $y_i$  at the slab interface, and various incidence angles  $\theta_i$  (with respect to the  $x$ -axis). The Gaussian-beam minimum spot-size is  $\sim 2.2a$  and the incidence point is located at the Rayleigh distance. (a)  $y_i = 0$ ,  $\theta_i = 10^\circ$ ; (b)  $y_i = -2.44a$ ,  $\theta_i = 10^\circ$ ; (c)  $y_i = -4.88a$ ,  $\theta_i = 10^\circ$ ; (d)  $y_i = 0$ ,  $\theta_i = 45^\circ$ ; (e)  $y_i = -2.44a$ ,  $\theta_i = 45^\circ$ ; (f)  $y_i = -4.88a$ ,  $\theta_i = 45^\circ$ ; (g)  $y_i = 0$ ,  $\theta_i = 60^\circ$ ; (h)  $y_i = -2.44a$ ,  $\theta_i = 60^\circ$  and (i)  $y_i = -4.88a$ ,  $\theta_i = 60^\circ$ .

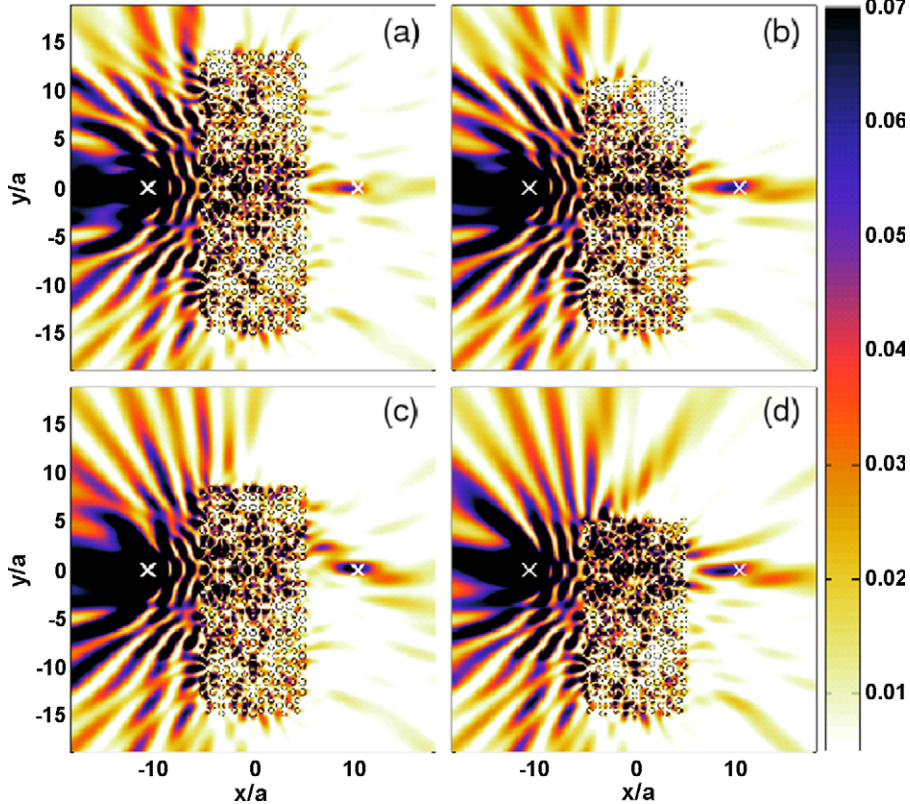


Fig. 7. As in Fig. 2(a), but for various asymmetric slab configurations with different lateral width  $h$ . (a)  $h = 29.4a$ ; (b)  $h = 26.7a$ ; (c)  $h = 23.9a$  and (d)  $h = 20.6a$ .

position ( $d_x = t/2$  and  $y = 0$ ). Results are shown in Fig. 7. In this case, the focus turns out to be rather stable, in spite of the  $x$ -symmetry breaking. These results clearly reveal the key role played in the focus formation by *short-range* interactions involving a neighborhood of

the parent tiling (highlighted via green full dots in Fig. 1(b)). This can be also observed considering a configuration where the slab lateral width is symmetrically reduced to  $\sim 11a$  with respect to the  $y$ -axis, as shown in Fig. 8. Again, in spite of the considerably reduced lateral width, the focusing properties associated to the symmetry local point located at  $(x = 0, y = 0)$  appear to be rather robust, as if their occurrence was restricted to a limited range of incidence angles. This renders these PQC structures particularly appealing for the development of compact optical systems.

#### 4. Conclusions

To sum up, a comprehensive parametric numerical study of the lensing properties of quasiperiodic dodecagonal PQC slabs has been carried out. Results confirm that these structures possess focusing properties in several frequency regions, even if critically associated to local symmetry points (and neighboring regions) existing in the tiling lattice. Indeed, our full-wave numerical simulations show that varying the slab thickness or the source position, the field distributions

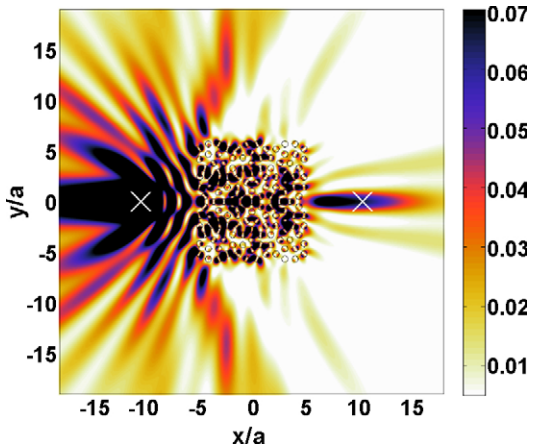


Fig. 8. As in Fig. 7, but reducing the lateral width to  $\sim 11a$  symmetrically with respect to the  $y$ -axis.

inside the slab and in the image plane change dramatically. The original interpretation in [26], within the framework of “effective negative refractive-index and evanescent wave amplification”, does not appear adequate to describe the underlying phenomenologies, which entail complex near-field scattering effects and short-range interactions. Nevertheless, this particular PQC shows some peculiarities in the EM response that deserve further investigation. In particular, applications to lenses with small aperture or antennas with highly directional beaming could be envisaged.

Also of interest it is the parametric study of the refraction and focusing properties of other classes of PQCs based on periodic (e.g., Archimedean [35]) and aperiodic (e.g., Penrose [19,22], octagonal [21], circular [36]) tilings characterized by diverse degrees of (local and/or statistical) rotational symmetry.

## Acknowledgements

This work has been funded by the Italian Ministry of Education and Scientific Research (MIUR) under the PRIN-2006 grant on “Study and realization of metamaterials for electronics and TLC applications”. The authors wish to thank the referees for their useful comments and suggestions, as well as Mr. V. De Luise and Mr. A. Micco for their technical support.

## References

- [1] E. Yablonovitch, Phys. Rev. Lett 58 (1987) 2059.
- [2] S. John, Phys. Rev. Lett. 58 (1987) 2486.
- [3] A. Shinya, S. Mitsugi, T. Tanabe, M. Notomi, I. Yokohama, H. Takara, S. Kawanishi, Opt. Express 14 (2006) 1230.
- [4] M. Notomi, Phys. Rev. B 62 (2000) 10696.
- [5] S. Foteinopoulou, C.M. Soukoulis, Phys. Rev. B 72 (2005) 165112.
- [6] W. Lu, S. Sridhar, Opt. Express 13 (2005) 10673.
- [7] C. Luo, S. Johnson, J. Joannopoulos, J. Pendry, Phys. Rev. B 65 (2002) 201104R.
- [8] P. Parimi, W. Lu, P. Vodo, S. Sridhar, Nature 426 (2003) 404.
- [9] E. Cubukcu, K. Aydin, E. Ozbay, S. Foteinopoulou, C.M. Soukoulis, Nature 423 (2003) 604.
- [10] T. Decoopman, G. Tayeb, S. Enoch, D. Maystre, B. Gralak, Phys. Rev. Lett. 97 (2006) 073905.
- [11] R. Moussa, T. Koschny, C. Soukoulis, Phys. Rev. B 74 (2006) 115111.
- [12] J.B. Pendry, Phys. Rev. B 85 (2000) 3966.
- [13] X. Wang, Z. Ren, K. Kempa, Opt. Express 12 (2004) 2919.
- [14] Z. Li, L. Lin, Phys. Rev. B 68 (2003) 245110.
- [15] D. Shechtman, I. Blech, D. Gratias, J.W. Cahn, Phys. Rev. Lett. 53 (1984) 1951.
- [16] D. Levine, P.J. Steinhardt, Phys. Rev. Lett. 53 (1984) 2477.
- [17] M. Senechal, Quasicrystals and Geometry, Cambridge University Press, Cambridge, UK, 1995.
- [18] M. Zoorob, M. Charleton, G. Parker, J. Baumberg, M. Netti, Nature 404 (2000) 740.
- [19] M. Kaliteevski, S. Brand, R. Abram, T. Krauss, R.D.L. Rue, P. Millar, Nanotechnology 11 (2000) 274.
- [20] M. Kaliteevski, S. Brand, R. Abram, T. Krauss, R.D.L. Rue, P. Millar, J. Mod. Opt. 47 (2000) 1771.
- [21] Y.S. Chan, C.T. Chan, Z. Liu, Phys. Rev. Lett. 80 (1998) 956.
- [22] A.D. Villa, S. Enoch, G. Tayeb, V. Pierro, V. Galdi, F. Capolino, Phys. Rev. Lett. 94 (2005) 183903.
- [23] M. Bayndir, E. Cubukcu, I. Bulu, E. Ozbay, Phys. Rev. B 63 (2001) 161104(R).
- [24] S. Cheng, L.-M. Li, C. Chan, Z. Zhang, Phys. Rev. B 59 (1999) 4091.
- [25] A. Della Villa, S. Enoch, G. Tayeb, F. Capolino, V. Pierro, V. Galdi, Opt. Express 14 (2006) 10021.
- [26] Z. Feng, X. Zhang, Y. Wang, Z. Li, B. Cheng, D.Z. Zhang, Phys. Rev. Lett. 94 (2005) 247402.
- [27] X. Zhang, Z. Li, B. Cheng, D. Zhang, Opt. Express 15 (2007) 1292.
- [28] X. Zhang, Phys. Rev. B 75 (2007) 024209.
- [29] M. Oxborrow, C. Henley, Phys. Rev. B 48 (1993) 6966.
- [30] D. Felbacq, G. Tayeb, D. Maystre, J. Opt. Soc. Am. A 11 (1994) 2526.
- [31] W. Kohn, N. Rostoker, Phys. Rev. 94 (1954) 1111.
- [32] L. Rayleigh, Philos. Mag. 34 (1992) 481.
- [33] A. Asatryan, K. Busch, R. McPhedran, L. Botten, M. de Sterke, N. Nicorovici, Phys. Rev. E 63 (2001) 046612.
- [34] A. Asatryan, S. Fabre, K. Busch, R. McPhedran, L. Botten, M. de Sterke, N. Nicorovici, Opt. Express 8 (2001) 191.
- [35] S. David, A. Chelnokov, J.-M. Lourtioz, IEEE J. Quant. Elect. 37 (2001) 1427.
- [36] S. Xiao, M. Qiu, Photonics Nanostruct. Fund. Appl. 3 (2005) 134.